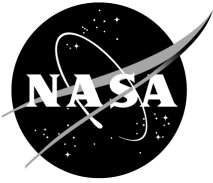


NASA/TM—2011–216455



# **Direct Visualization of Shock Waves in Supersonic Space Shuttle Flight**

*J.M. O'Farrell*

*United Space Alliance, Huntsville, Alabama*

*T.J. Rieckhoff*

*Marshall Space Flight Center, Marshall Space Flight Center, Alabama*

---

*January 2011*

## The NASA STI Program...in Profile

Since its founding, NASA has been dedicated to the advancement of aeronautics and space science. The NASA Scientific and Technical Information (STI) Program Office plays a key part in helping NASA maintain this important role.

The NASA STI Program Office is operated by Langley Research Center, the lead center for NASA's scientific and technical information. The NASA STI Program Office provides access to the NASA STI Database, the largest collection of aeronautical and space science STI in the world. The Program Office is also NASA's institutional mechanism for disseminating the results of its research and development activities. These results are published by NASA in the NASA STI Report Series, which includes the following report types:

- **TECHNICAL PUBLICATION.** Reports of completed research or a major significant phase of research that present the results of NASA programs and include extensive data or theoretical analysis. Includes compilations of significant scientific and technical data and information deemed to be of continuing reference value. NASA's counterpart of peer-reviewed formal professional papers but has less stringent limitations on manuscript length and extent of graphic presentations.
- **TECHNICAL MEMORANDUM.** Scientific and technical findings that are preliminary or of specialized interest, e.g., quick release reports, working papers, and bibliographies that contain minimal annotation. Does not contain extensive analysis.
- **CONTRACTOR REPORT.** Scientific and technical findings by NASA-sponsored contractors and grantees.
- **CONFERENCE PUBLICATION.** Collected papers from scientific and technical conferences, symposia, seminars, or other meetings sponsored or cosponsored by NASA.
- **SPECIAL PUBLICATION.** Scientific, technical, or historical information from NASA programs, projects, and mission, often concerned with subjects having substantial public interest.
- **TECHNICAL TRANSLATION.** English-language translations of foreign scientific and technical material pertinent to NASA's mission.

Specialized services that complement the STI Program Office's diverse offerings include creating custom thesauri, building customized databases, organizing and publishing research results...even providing videos.

For more information about the NASA STI Program Office, see the following:

- Access the NASA STI program home page at <<http://www.sti.nasa.gov>>
- E-mail your question via the Internet to <[help@sti.nasa.gov](mailto:help@sti.nasa.gov)>
- Fax your question to the NASA STI Help Desk at 443-757-5803
- Phone the NASA STI Help Desk at 443-757-5802
- Write to:  
NASA STI Help Desk  
NASA Center for AeroSpace Information  
7115 Standard Drive  
Hanover, MD 21076-1320

NASA/TM—2011–216455



# **Direct Visualization of Shock Waves in Supersonic Space Shuttle Flight**

*J.M. O'Farrell*

*United Space Alliance, Huntsville, Alabama*

*T.J. Rieckhoff*

*Marshall Space Flight Center, Marshall Space Flight Center, Alabama*

National Aeronautics and  
Space Administration

Marshall Space Flight Center • MSFC, Alabama 35812

---

*January 2011*

## Acknowledgments

The authors would like to thank Jeff Hixson (USA), Gretchen Hartwog, Jessica Coleman (USA), Phil Peterson (Boeing), and Karla Bundy Fay (USA) for their help in obtaining mission imagery and data for missions STS-110 and STS-114 and their editorial comments and review of this Technical Memorandum. Also, we would like to thank the NASA Space Shuttle Imagery Integration Group, Brenda Eliason, Beth St. Peter, and Dave Melendrez for their helpful review and comments.

Available from:

NASA Center for AeroSpace Information  
7115 Standard Drive  
Hanover, MD 21076-1320  
443-757-5802

This report is also available in electronic form at  
<<https://www2.sti.nasa.gov>>

## TABLE OF CONTENTS

1. INTRODUCTION .....	1
2. SPACE SHUTTLE VEHICLE WB-57 ASCENT VIDEO EXPERIMENT IMAGERY .....	2
3. SPACE SHUTTLE VEHICLE GROUND CAMERA IMAGERY .....	8
4. OBSERVATIONS ON SHOCK BOUNDARIES .....	17
4.1 Order of Appearance .....	17
4.2 Amount of Refraction .....	17
4.3 Multiple Linear Optical Distortions Visible .....	19
4.4 Ripples in a Shock Boundary .....	19
4.5 Other Observations of Linear Optical Distortion .....	21
5. DISCUSSION .....	23
REFERENCES .....	25

## LIST OF FIGURES

1.	STS-114 and STS-110 SSV Mach number profiles during ascent .....	2
2.	STS-114 condensation collar formation at 41.45 s MET .....	3
3.	STS-114 shock structure at 50.87 s MET .....	3
4.	STS-114 shock structure at 52.67 s MET .....	4
5.	STS-114 shock structure at 54.64 s MET .....	4
6.	STS-114 shock structure at 55.49 s MET .....	5
7.	STS-114 shock structure at 59.72 s MET .....	5
8.	STS-114 shock structure at 59.82 s MET .....	6
9.	STS-114 shock structure at 62.99 s MET .....	6
10.	Camera E207 location .....	8
11.	STS-110 trajectory from BET data .....	9
12.	STS-110 shock at 59 s MET .....	10
13.	STS-110 shock at 59.002 s MET .....	10
14.	STS-110 shock at 59.005 s MET .....	10
15.	STS-110 shock at 59.007 s MET .....	10
16.	STS-110 shock at 59.010 s MET .....	11
17.	STS-110 shock at 59.012 s MET .....	11
18.	STS-110 shock at 59.015 s MET .....	11
19.	STS-110 shock at 59.017 s MET .....	11
20.	Camera E207 view angle versus chock cone angle .....	12

## LIST OF FIGURES (Continued)

21.	STS-110 shock sheath at 50 s MET .....	13
22.	STS-10 shock sheath at 55 s MET .....	13
23.	STS-110 shock sheath at 60 s MET .....	14
24.	STS-110 shock sheath at 60 s MET .....	14
25.	STS-110 shock sheath at 70 s MET .....	15
26.	STS-110 shock sheath at 100 s MET .....	15
27.	STS-110 LODs at (a) 55 s and (b) 60 s MET .....	17
28.	STS-110 SSME No. 1 nozzle refracted through shock boundary layer: (a) Actual SSME diameter (blue arrow) and (b) bending due to refraction (red arrow) .....	18
29.	View angle effect on LOD .....	18
30.	Multiple LODs visible .....	19
31.	Refraction direction illustrates ripples in the shock boundary .....	20
32.	Minor ripples in the shock boundary: (a) Noted at a time prior to the time for (b) ...	20
33.	STS-116 SSME refraction: (a) Shock boundary visible in SRB plumes and (b) shock boundary visible as moving points of light .....	21
34.	STS-107 shock boundaries (LODs) .....	22

## LIST OF ACROMYMS AND SYMBOLS

BET	best estimated trajectory
ET	external tank
LOD	linear optical distortion
MET	mission elapsed time
NSTS	National Space Transportation System
RCC	reinforced carbon-carbon
SRB	solid rocket booster
SSME	space shuttle main engine
SSP	space shuttle program
SSV	space shuttle vehicle
STS	space transportation system
TM	Technical Memorandum
UCS	universal camera site
WAVE	WB-57 ascent video experiment

## TECHNICAL MEMORANDUM

### DIRECT VISUALIZATION OF SHOCK WAVES IN SUPERSONIC SPACE SHUTTLE FLIGHT

#### 1. INTRODUCTION

Schlieren photography, a method of imaging localized changes of refractive index in transparent media, has been the traditional shock wave visualization tool for supersonic vehicles.<sup>1,2</sup> As noted by Weinstein,<sup>2</sup> direct observation of shock boundaries is rare. This Technical Memorandum (TM) describes an instance of direct observation of shock waves produced on the space shuttle vehicle (SSV) during Space Transportation System (STS) ascent imagery provided by NASA tracking cameras that are used to track the SSV.<sup>3</sup>

Shock waves produced on the SSV form in the shape of a cone due to the geometry of the vehicle. The primary shock forms a bow shock at the nose of the vehicle while successive shock waves form in its wake. During SSV ascent, the density of air decreases outside of the shock cone while the air inside the cone compresses into a higher density. The abrupt density change over the shock boundary causes the light passing through the boundary to be refracted. Likewise, if atmospheric moisture is present during SSV ascent, condensation provides a visible counterpart to the acoustic shock wave being generated. Both circumstances have been captured by SSV ascent imagery and are presented.

As shock waves form around the SSV, the waves move away from the vehicle at the speed of sound. If viewed from a position on a plane reasonably orthogonal to the vehicle during ascent, the shock boundaries are often visible as linear structures emanating aftward from the vehicle. This type of visualization, while rare, is analogous to Schlieren photography of shock boundaries. Imagery from STS-114 illustrates this type of shock boundary visualization.

Viewed from a fixed position on the ground, shock boundaries may also become visible as they intersect the view angle of a tracking camera. In this case, the shock boundaries become visible by refracting light from the illuminated SSV structure and plumes in the background. The shock boundary is observed in the ascent imagery as an illuminated linear structure moving through the field of view and is noted as a linear optical distortion (LOD) during photographic analysis reporting of the mission. Imagery from STS-110 illustrates this type of shock boundary visualization. The visualization of shock boundaries as LODs is a common observation noted on many shuttle missions.

## 2. SPACE SHUTTLE VEHICLE WB-57 ASCENT VIDEO EXPERIMENT IMAGERY

Return-to-Flight was a time of heightened awareness of how vulnerable the SSV could be to ascent debris. STS-114 was the first launch after the 2003 loss of Space Shuttle *Columbia* and additional resources were obtained across the entire space shuttle program (SSP) to prevent a recurrence of the events that led to the loss of *Columbia*. In addition to the traditional ground tracking cameras, a new high-altitude airborne camera called the WB-57 ascent video experiment (WAVE) was used to capture SSV imagery during ascent. One anticipated benefit of the WAVE was the ability to capture imagery of the SSV even when thick cloud cover obscured the ground camera views. During STS-114, the vehicle passed through several light cloud layers and shock waves propagating from the vehicle were captured by the WAVE camera. Once the vehicle was above the cloud layers, the shock boundaries were no longer visible in the WAVE imagery. The visibility of shock boundaries depends on lighting, atmospheric, and viewing conditions.

The SSV Mach number can be plotted against mission elapsed time (MET) for a specific mission by using the wind relative Mach number profile acquired from the National Space Transportation System (NSTS) database, as is done for STS-114 and STS-110 in figure 1. Imagery from STS-114 of the shock boundary formation over an elapsed period of time is shown in figures 2–9. Using MET obtained directly from imagery and the plot provided in figure 1, the Mach number of the vehicle can then be determined.

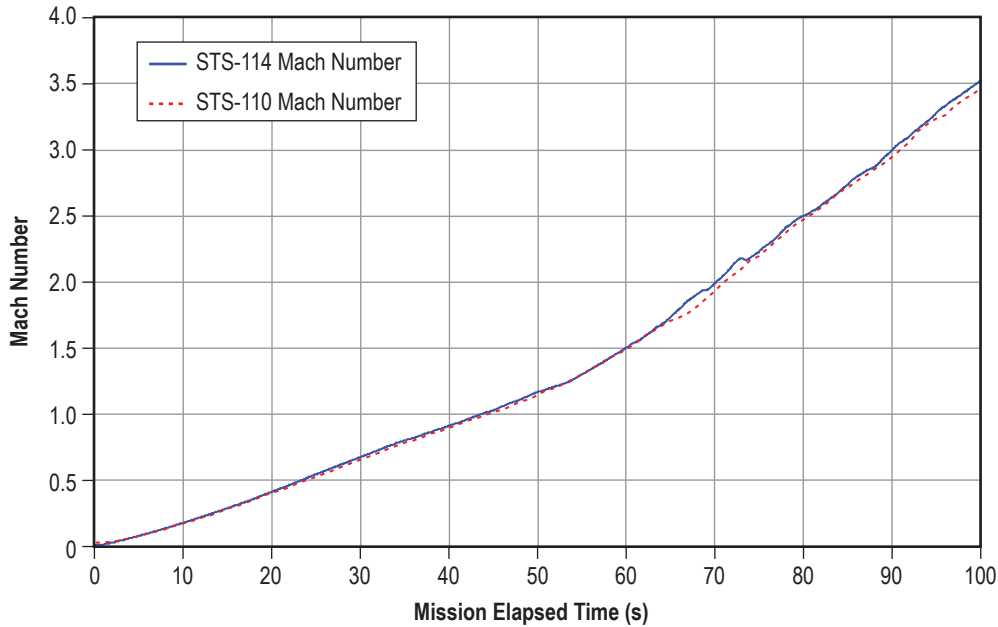


Figure 1. STS-114 and STS-110 SSV Mach number profiles during ascent.

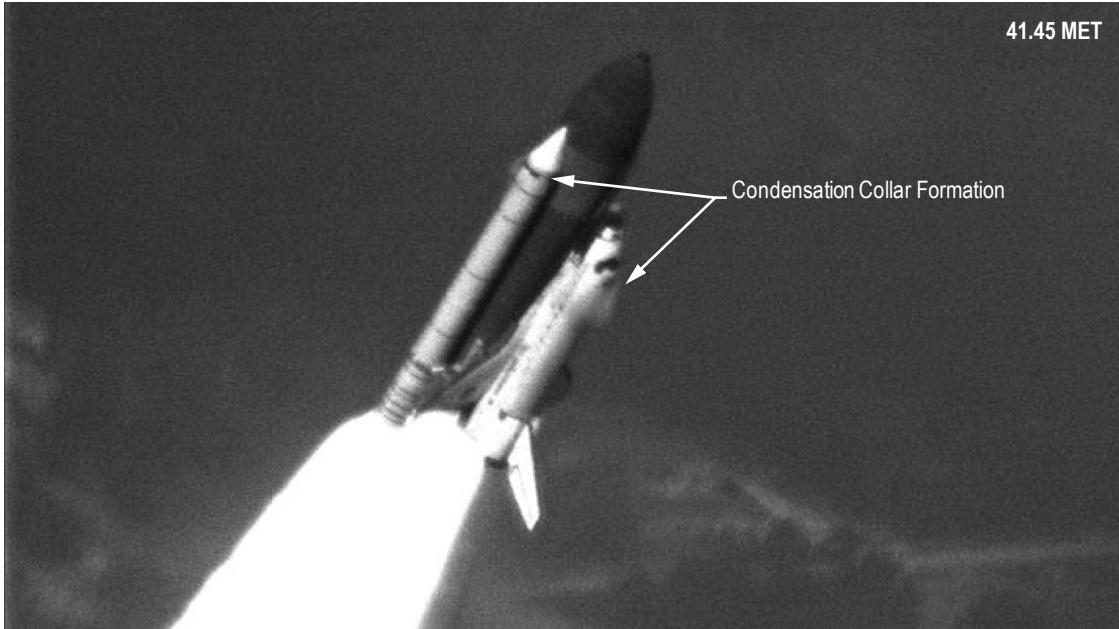


Figure 2. STS-114 condensation collar formation at 41.45 s MET.

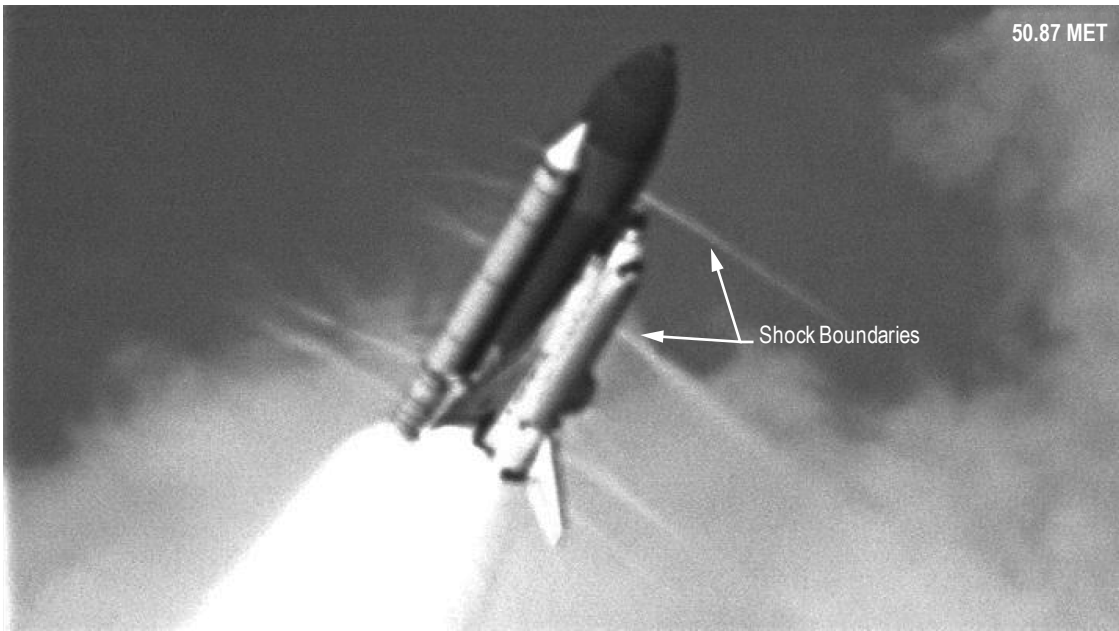


Figure 3. STS-114 shock structure at 50.87 s MET.

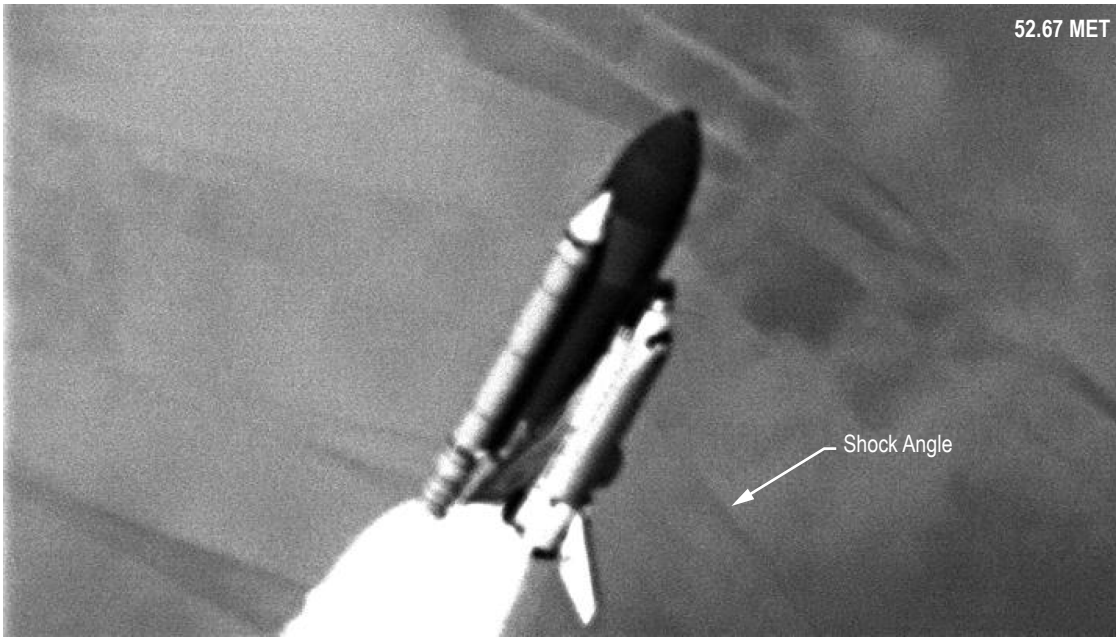


Figure 4. STS-114 shock structure at 52.67 s MET.



Figure 5. STS-114 shock structure at 54.64 s MET.

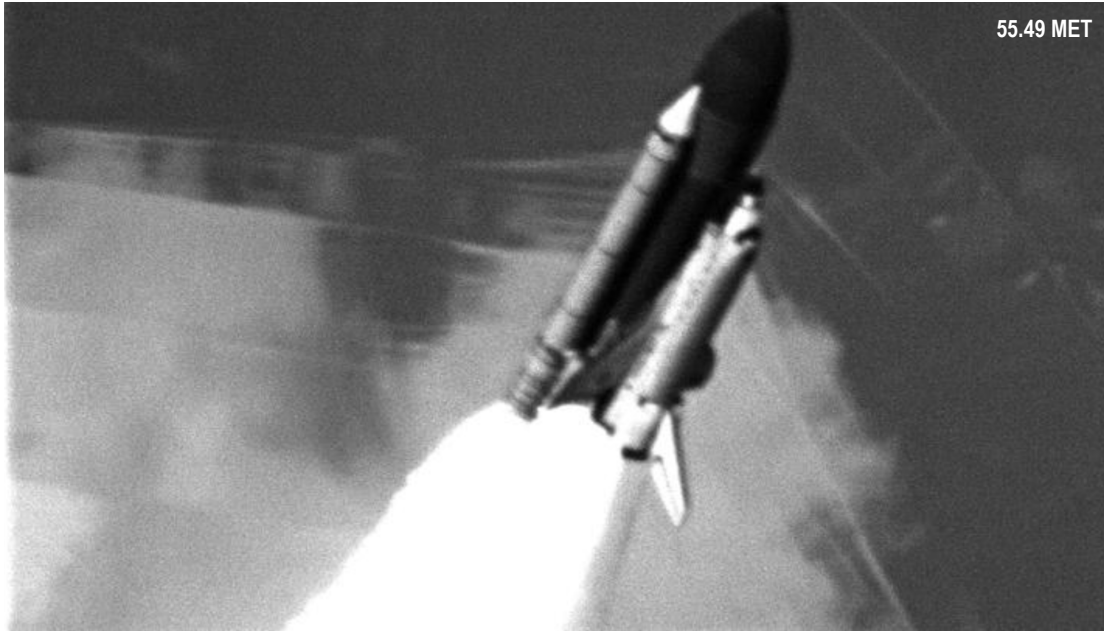


Figure 6. STS-114 shock structure at 55.49 s MET.



Figure 7. STS-114 shock structure at 59.72 s MET.

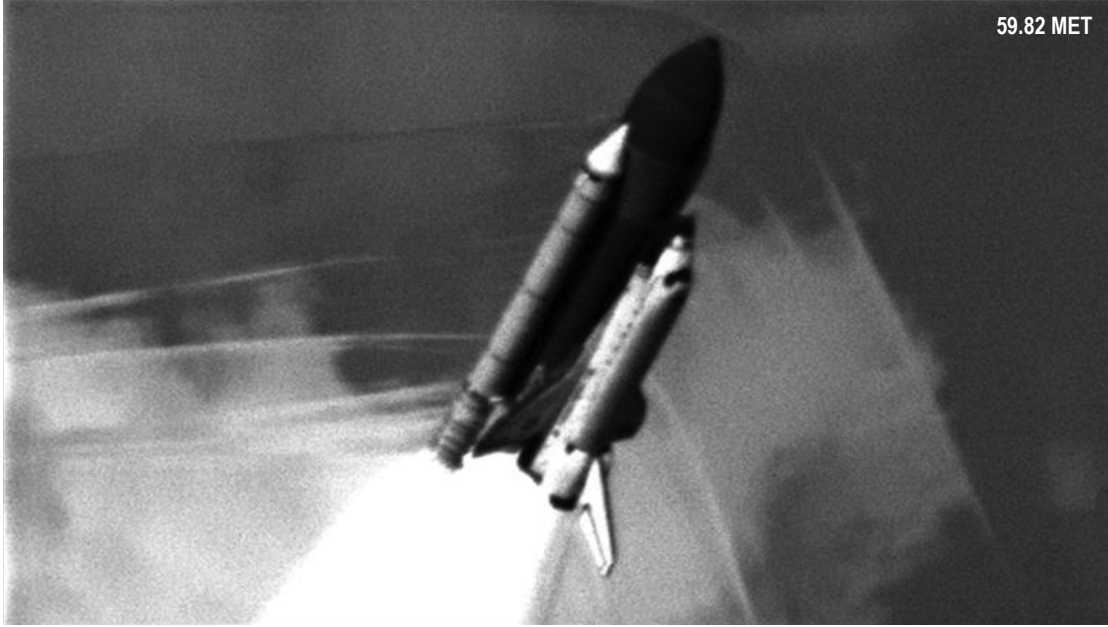


Figure 8. STS-114 shock structure at 59.82 s MET.



Figure 9. STS-114 shock structure at 62.99 s MET.

A condensation collar is first observed to form at the forward areas of the solid rocket boosters (SRBs), external tank (ET), and orbiter at  $\approx 41$  s MET (fig. 2). The condensation collar is a result of the pressure change at the shock boundary. Given sufficient humidity, condensation of the available moisture provides a visible counterpart to the acoustic shock wave being generated. Depending on atmospheric conditions, the condensation collars typically form just prior to the vehicle attaining Mach 1.0. For STS-114, the Mach number was  $\approx 0.95$  when the condensation collars were first observed to form.

As the Mach number increases, the shock angle to the vehicle becomes more acute. The bow shock and the structure of the secondary shocks from vehicle protuberances are clearly visible (fig. 7).

### 3. SPACE SHUTTLE VEHICLE GROUND CAMERA IMAGERY

Long-range tracking camera E207, located at Universal Camera Site-10, is  $\approx 5$  mi to the north and 2 mi to the west of the space shuttle launch site on pad 39-B (fig. 10). This 35-mm film camera is equipped with a 400-in focal length lens, which provides a close-up view of the aft area of the orbiter through SRB separation.

During STS-110, long-range ground cameras tracked the SSV from lift-off through separation of the SRBs from the orbiter and ET. Separation of the SRBs occurs  $\approx 2$  min after lift-off. For this particular mission, the sky was clear, providing excellent conditions for viewing the SSV during ascent. The vehicle traversed a trajectory determined from best estimated trajectory (BET) data as shown in figure 11.

At  $\approx 44$  s MET, the SSV attained Mach 1.0. At  $\approx 59$  s MET, as the vehicle approached Mach 1.45, a distinct shock boundary appeared in the imagery from ground camera E207. Although the shock boundaries are visible in several ground cameras, camera E207 imagery was chosen to illustrate shock boundary in this TM because it has resolution sufficient to demonstrate many of the interesting shock boundary features.

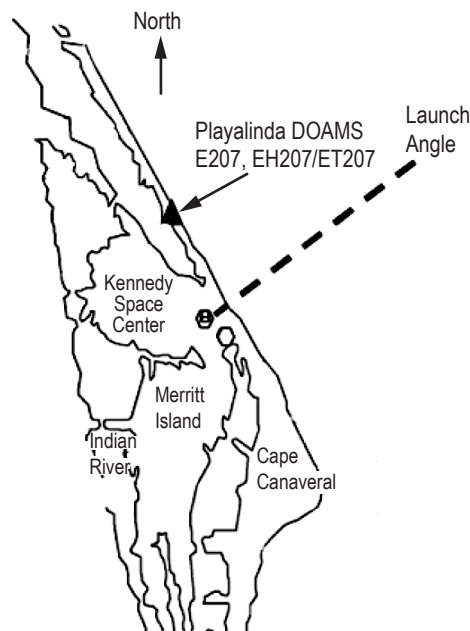


Figure 10. Camera E207 location.

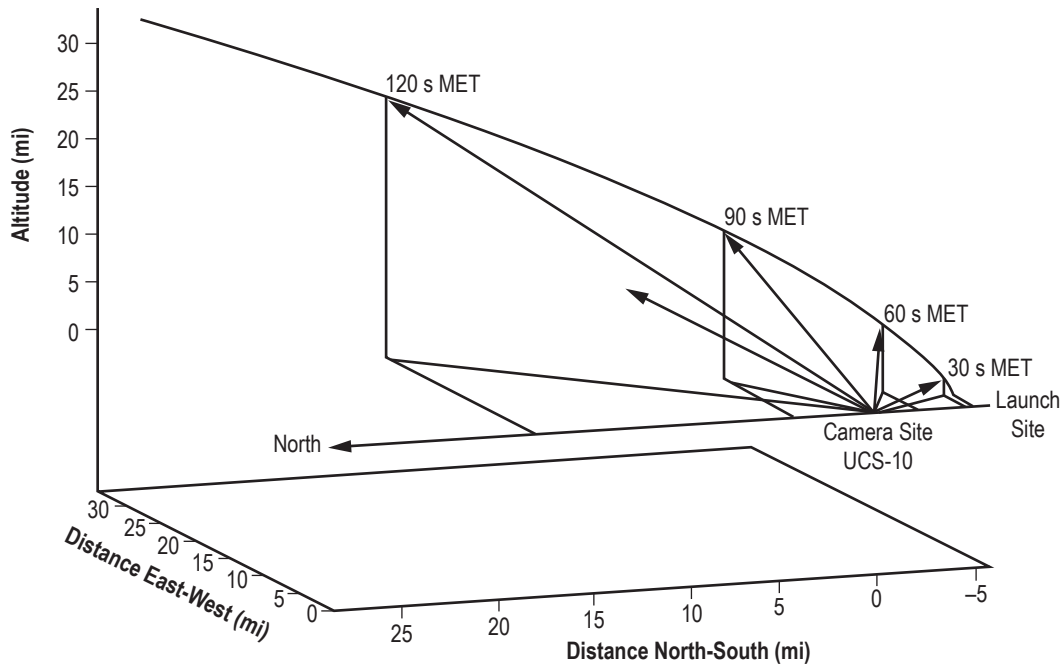


Figure 11. STS-110 trajectory from BET data.

The initial observation of a shock boundary is dependent on the location of the camera relative to the forming shock cone and other ground cameras may initially observe shock boundaries at a time different from that of camera E207. Shock boundaries may be visible up to and occasionally after SRB separation.

During the STS-110 mission, direct visualization of the shock boundary between the camera and the vehicle was possible due to the refraction of light at the shock boundary. The vehicle was illuminated by SRB exhaust plumes and provided the required lighting to enhance the difference at the shock boundary in the imagery.

In figures 12–19, a shock appeared approximately midway along the orbiter body and traveled nearly perpendicular to the axial direction of the vehicle in the image. The shock boundary moved aft of the SSV in the field of view, disappearing from camera view in the SRB plumes. Figure 13 clearly shows ripples in the shock boundary. All of the images show the bending of light due to refraction through the high-density shock layer. It is interesting to note that the shock boundaries that are visible are the same color as the original area of refracted light.

Also in this imagery, several shock boundaries can be observed in one frame. These boundaries are due to shocks that arise from vehicle protuberances and also from fluctuations of particular boundaries. Short video clips of the shock boundaries in motion are available at the Marshall Space Flight Center engineering photographic analysis Web site.<sup>4</sup> In the videos, the fluctuating shock boundaries can clearly be observed.

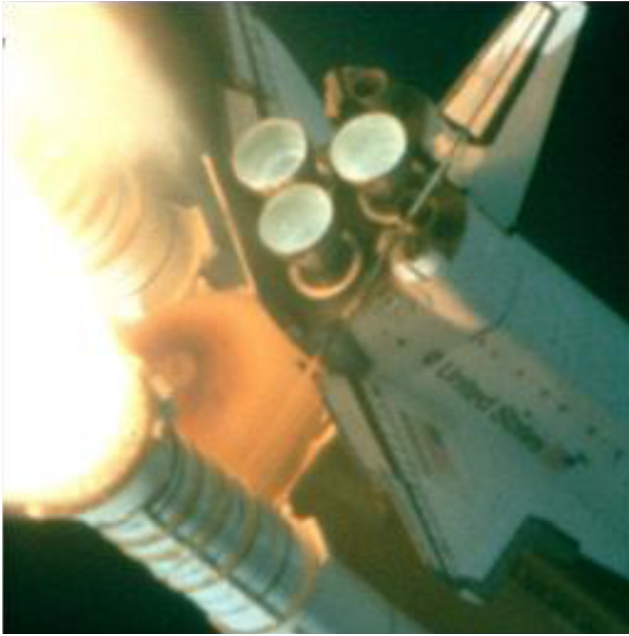


Figure 12. STS-110 shock at 59 s MET.

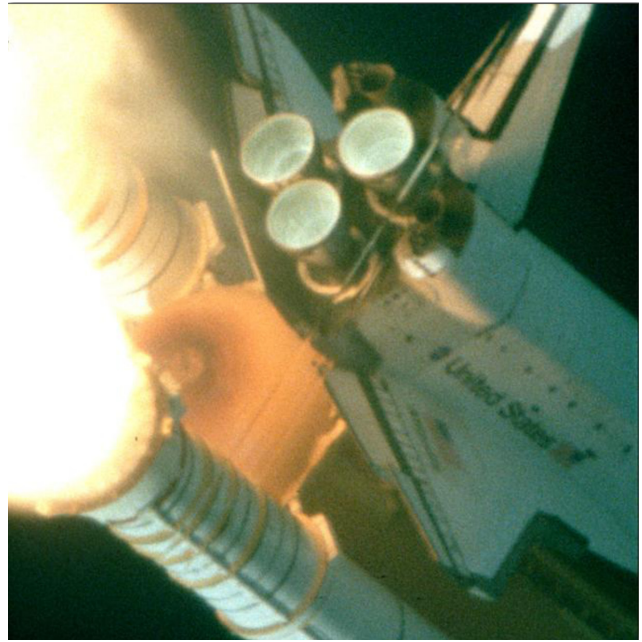


Figure 13. STS-110 shock at 59.002 s MET.

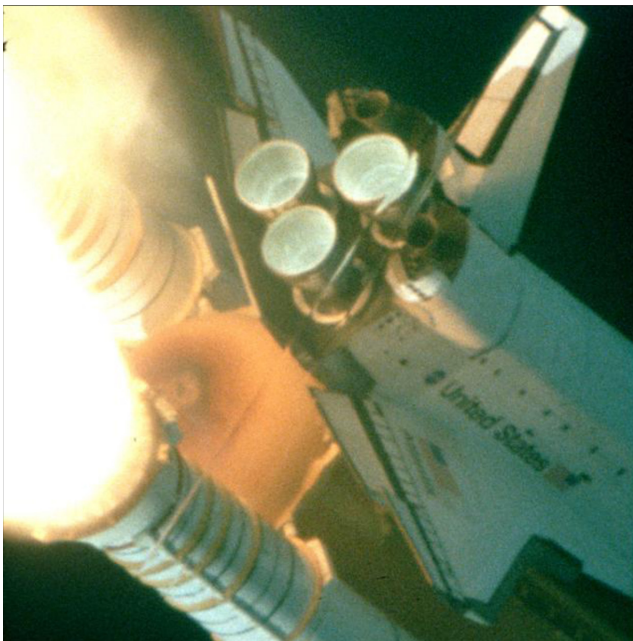


Figure 14. STS-110 shock at 59.005 s MET.

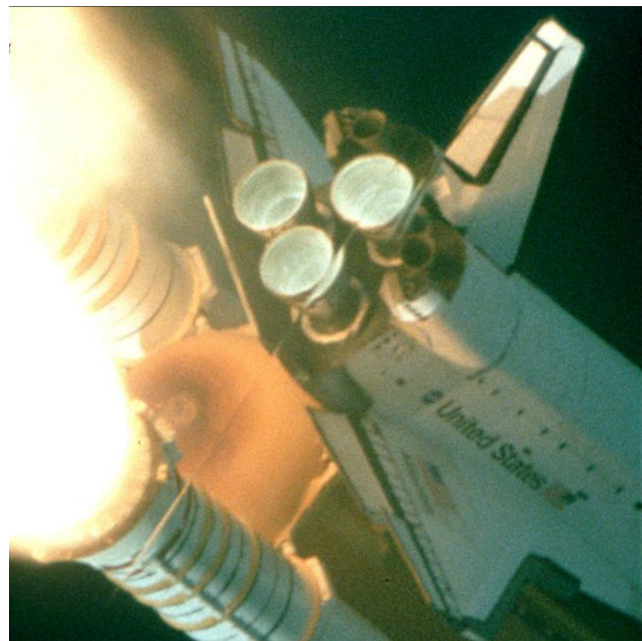


Figure 15. STS-110 shock at 59.007 s MET.

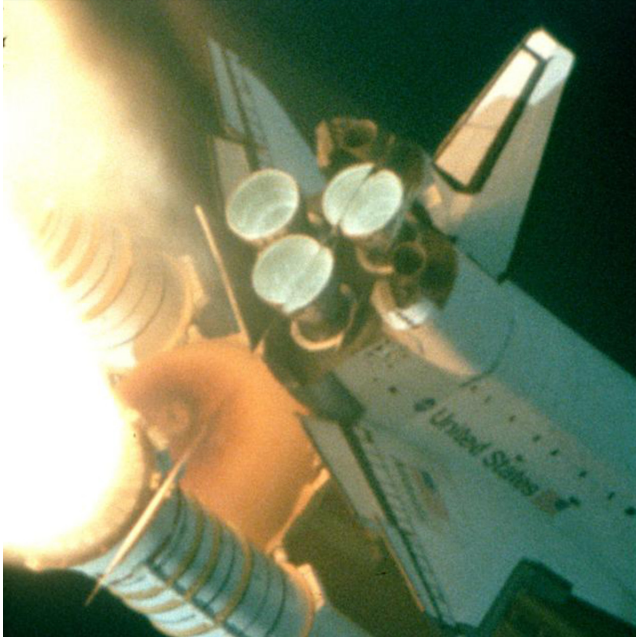


Figure 16. STS-110 shock at 59.010 s MET.

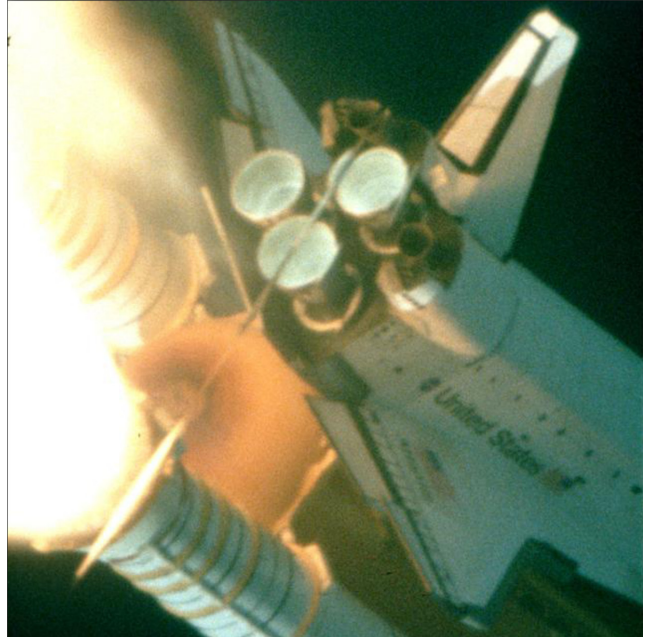


Figure 17. STS-110 shock at 59.012 s MET.

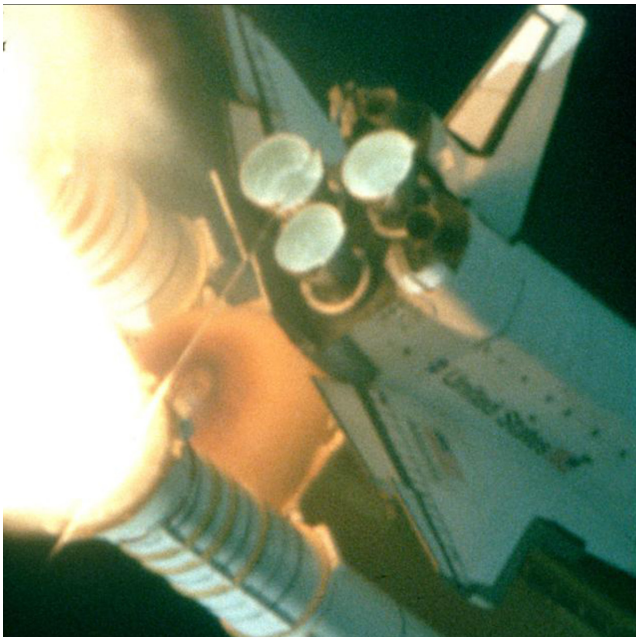


Figure 18. STS-110 shock at 59.015 s MET.

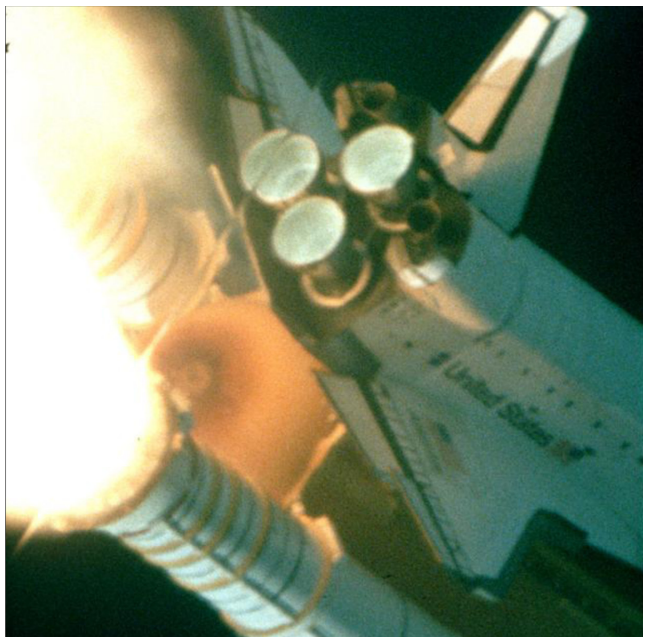


Figure 19. STS-110 shock at 59.017 s MET.

The shock wave from a supersonic object is a cone formed from overlapping spherical wavefronts. As each of these wavefronts forms, it propagates radially outward at the speed of sound, forming a shock cone.

The view angle, the angle from the SSV trajectory to the tracking camera’s principal axis, can be calculated using the BET data from the NSTS database. The shock cone angle, the angle between the vehicle and the shock boundary, is calculated using the oblique shock relations for a Mach 1.45 airflow. The relationship between the view angle and the shock cone angle versus the MET is shown in figure 20. When the shock cone angle is equal to the view angle, an observer at the camera site would be looking directly at the shock boundary. At  $\approx 55$  s MET, the shock cone angle and the view angle are nearly equal. It is during this time that the LODs become visible. The Mach number for STS-110 is shown in figure 1 for reference (dotted line).

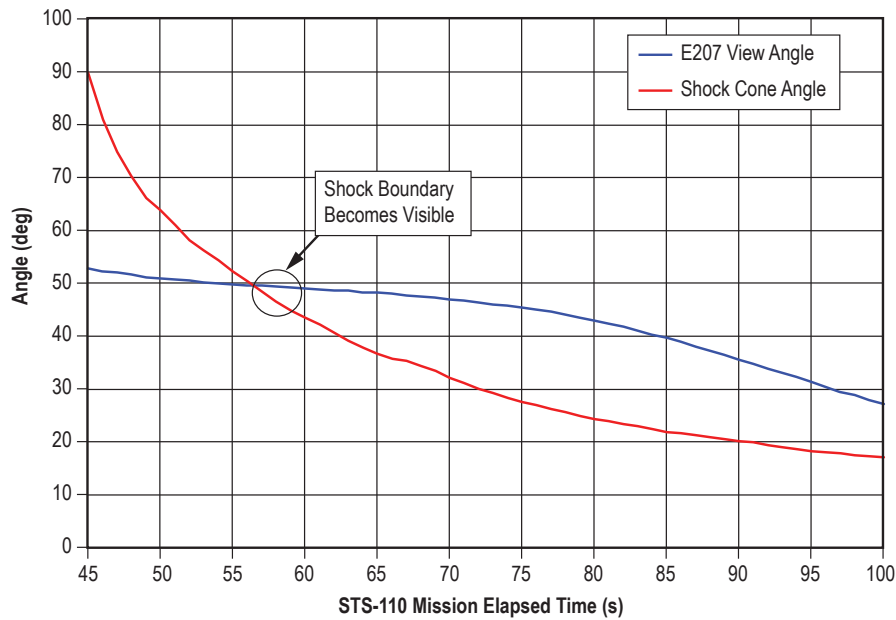


Figure 20. Camera E207 view angle versus chock cone angle.

As the SSV ascends and attains Mach 1.0, shock waves form and travel away from the vehicle at the speed of sound. During that time, LODs are observed as shock waves passing through the view of the long-range ground tracking camera. At several instances in time, the geometry of the shock cone and the line of sight were modeled in MATLAB using the STS-110 trajectory and theoretical sound speed at the corresponding altitude and are shown in progression in figures 21–26.

In the following graphs, the black curve is the trajectory of the SSV, the red line is the line of sight from camera E207 to the SSV at the time indicated, and the conical structure is the spread of the sonic shock boundary. In the early MET images (figs. 21 and 22), the conical shock sheath has grown little and the line of sight from the camera to the orbiter does not intersect the shock sheath. At 60 s MET, the simulation estimates that the shock sheath has intersected the camera line of sight as shown in figures 23 and 24.

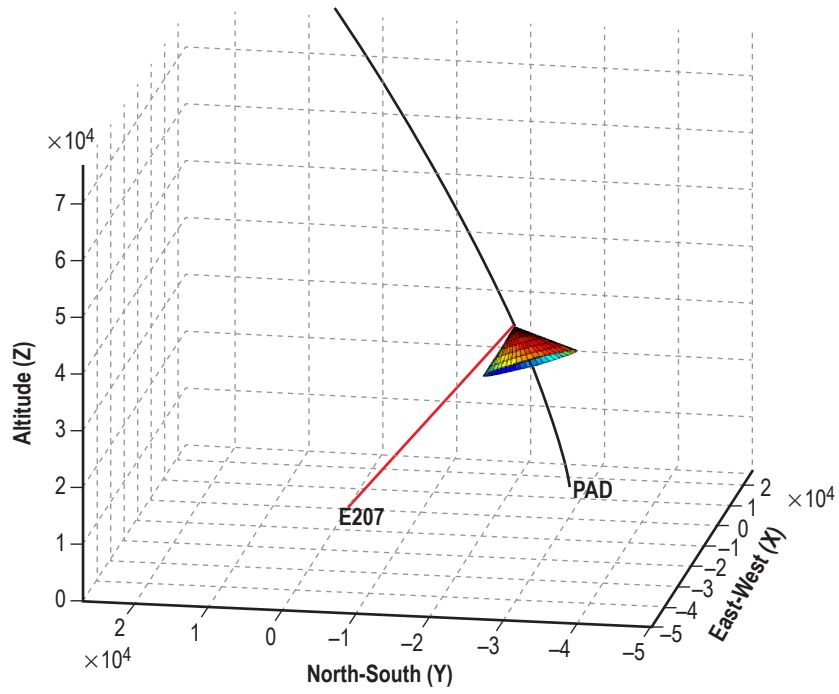


Figure 21. STS-110 shock sheath at 50 s MET.

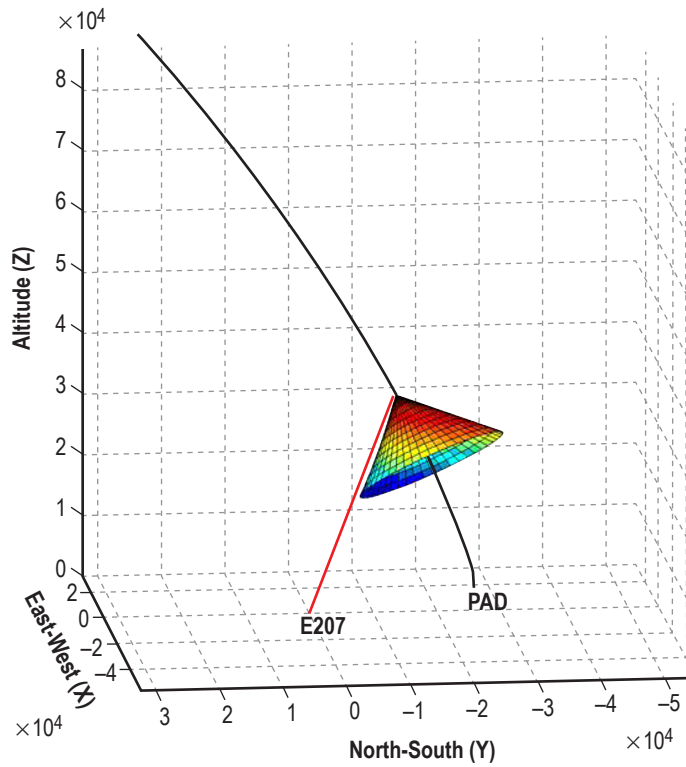


Figure 22. STS-10 shock sheath at 55 s MET.

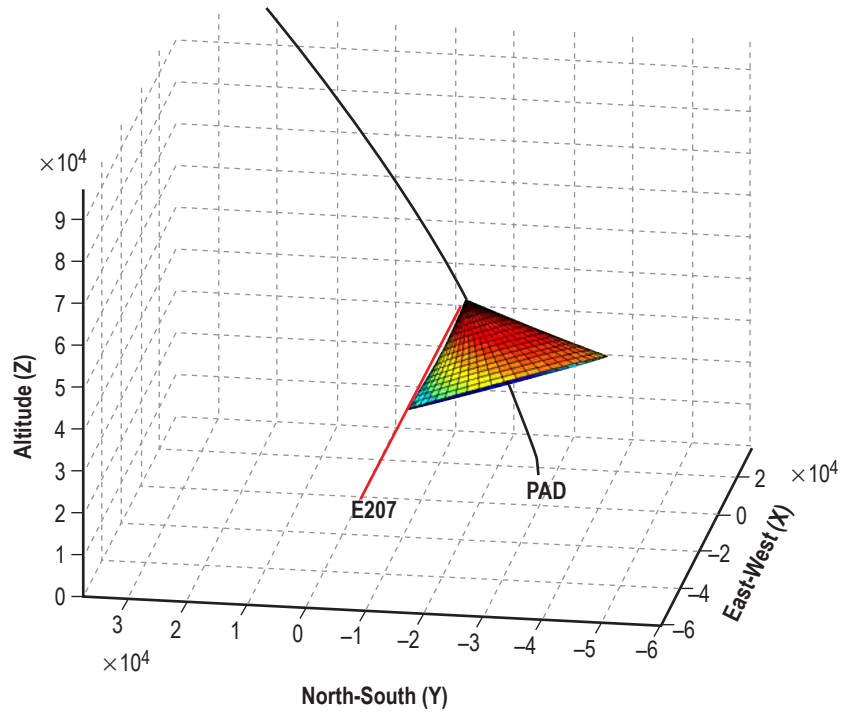


Figure 23. STS-110 shock sheath at 60 s MET.

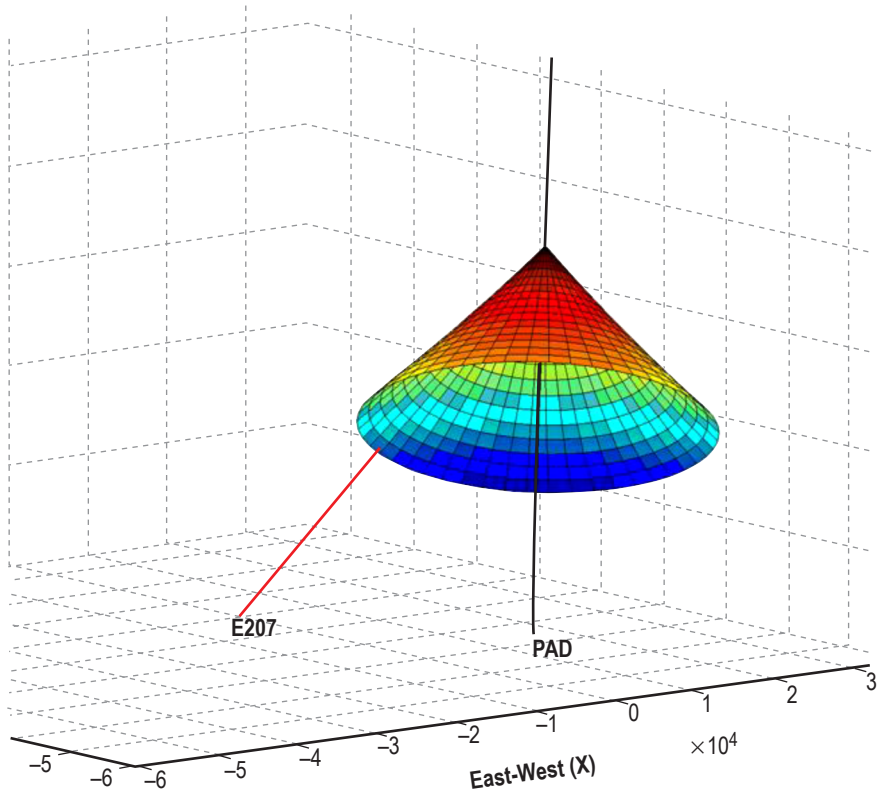


Figure 24. STS-110 shock sheath at 60 s MET.

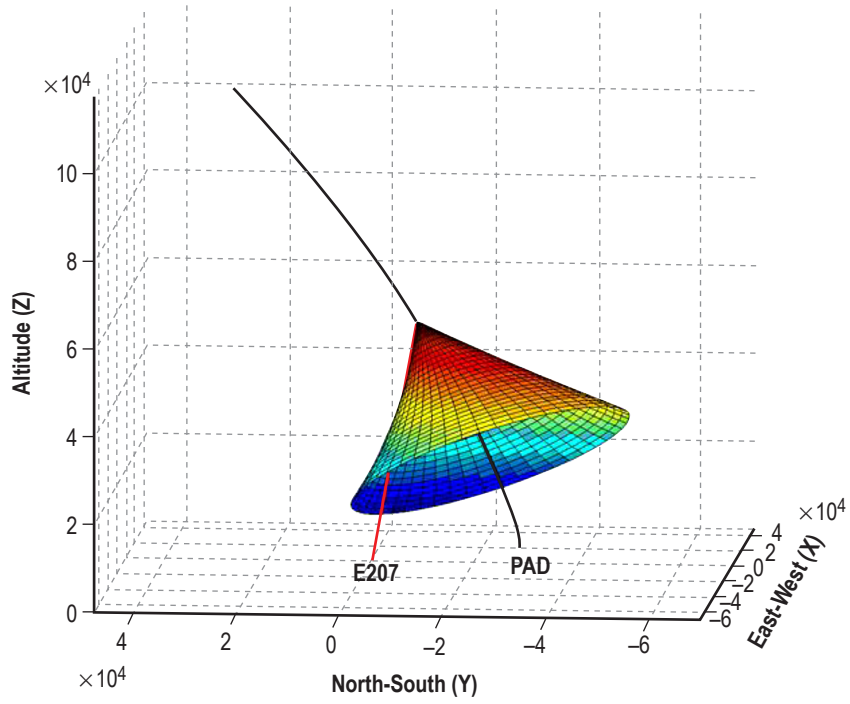


Figure 25. STS-110 shock sheath at 70 s MET.

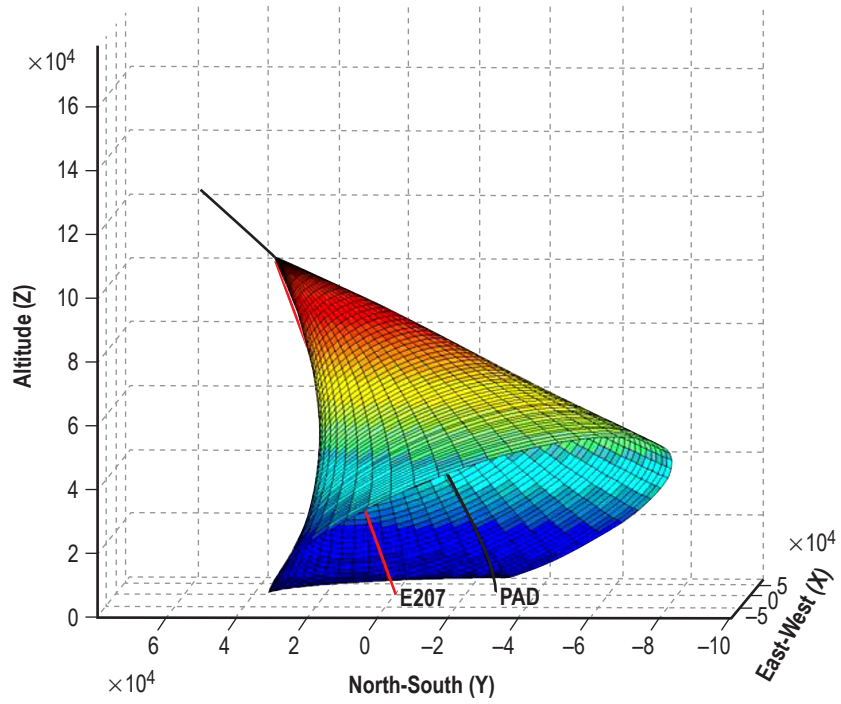


Figure 26. STS-110 shock sheath at 100 s MET.

The MATLAB simulation uses theoretical data for atmospheric parameters determining the speed of sound at the corresponding altitude; therefore, the model will not give precise intersection data for missions when the line of sight intersects the sheath boundary. However, the simulation places the intersection in approximately the correct timeframe. Typically, the LODs are first observed around 55–60 s MET. Prior to 55 s MET, the line of sight precedes the growing shock sheath and after 60 s MET, the line of sight clearly intersects the shock sheath.

## 4. OBSERVATIONS ON SHOCK BOUNDARIES

There are several interesting observed effects of the LODs. These include the order of appearance, the amount of refraction, multiple LODs, ripples in the shock boundary, and some observational effects of LODs.

### 4.1 Order of Appearance

Often several LODs are observed during ascent and many times there are several visible at once. LODs typically appear on the vehicle body and move aft. The first LOD is noted at  $\approx 55$  s MET. A late occurring LOD often appears and travels aft at  $\approx 60$  s. The time of appearance is thought to be related to a particular shock boundary. It is thought that the 55 s MET LOD is probably related to the aft shock from the tail of the vehicle and the 60 s MET LOD could be related to the bow shock of the vehicle. These two shocks are illustrated in figure 27.

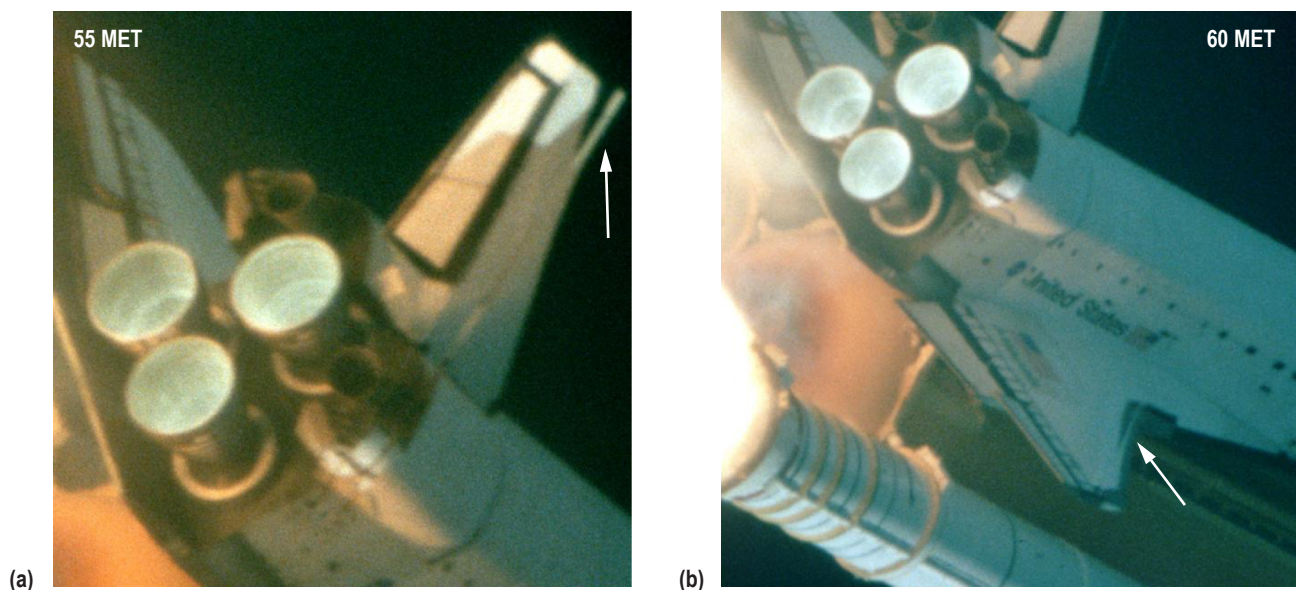


Figure 27. STS-110 LODs at (a) 55 s and (b) 60 s MET.

### 4.2 Amount of Refraction

Due to the density differences on opposite sides of the shock boundary, refraction of light will occur. When utilizing imagery for object measurement and/or identification, care must be taken to account for the shift in object location due to refraction at the shock boundary. Measurement errors across shock boundaries may be quite significant. In STS-110 imagery from camera E207, as shown in figure 28, the position of one edge of the space shuttle main engine (SSME) nozzle

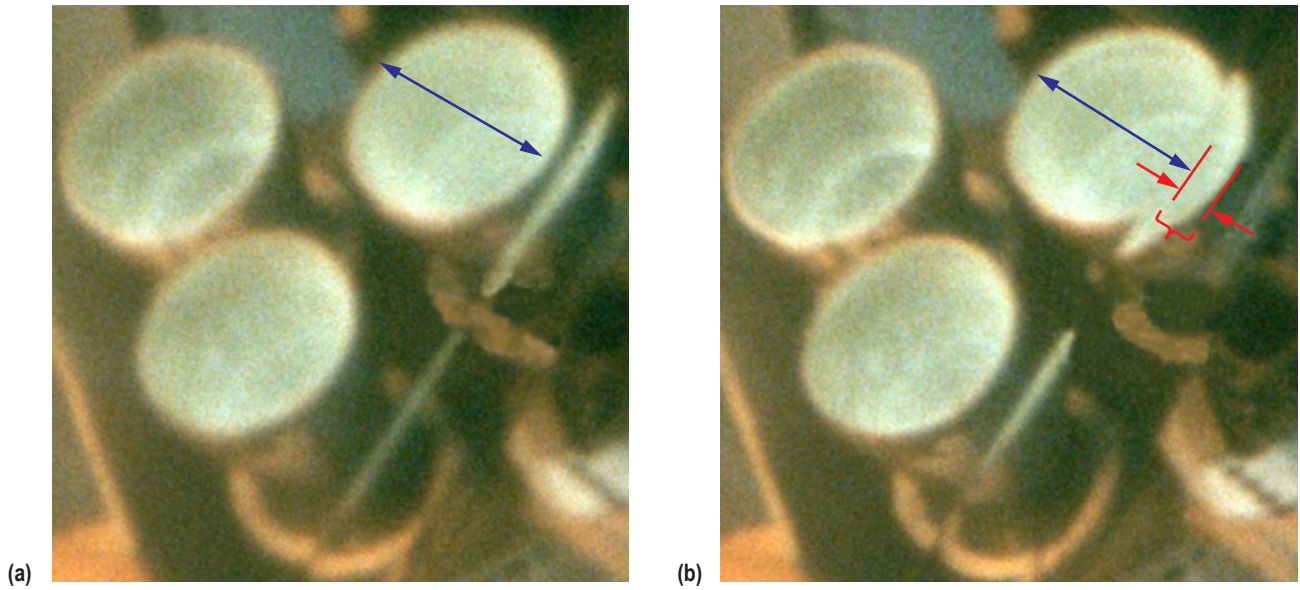


Figure 28. STS-110 SSME No. 1 nozzle refracted through shock boundary layer: (a) Actual SSME diameter (blue arrow) and (b) bending due to refraction (red arrow).

No. 1 has shifted by nearly 20% of the actual diameter or about 20 in. This gives an indication of the amount of pixel shift necessary to make measurements across the shock boundary at the particular time the image was obtained.

The view angle to the vehicle also shifts the observed position through a shock boundary. This may be observed as a discontinuity in the continuous orbiter body flap structure (fig. 29).

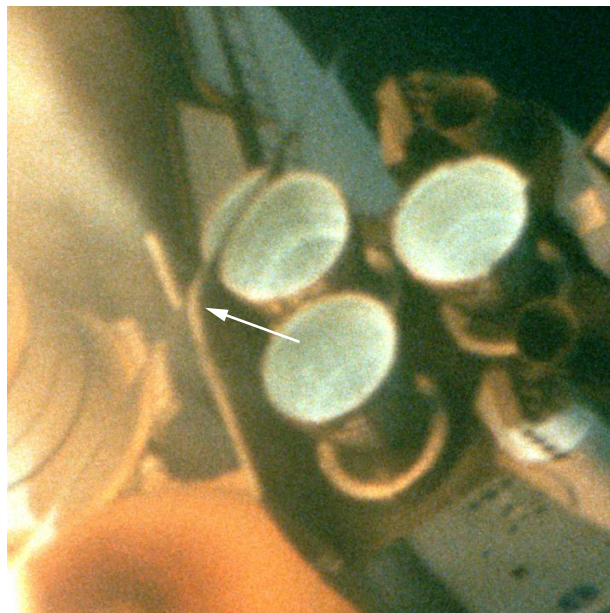


Figure 29. View angle effect on LOD.

### 4.3 Multiple Linear Optical Distortions Visible

Often multiple LODs are visible. Typically, a particular shock boundary may be distinguished by a group of LODs that travel together. Four groups were noted in figure 30. Although the LODs in each group move together, it is unknown whether separately these groups are associated with one shock or with multiple shock boundaries. The LODs are often difficult to track for extended periods since they become washed out by the brightness of the SRB plumes or indistinct from the background as they travel forward where the amount of light reflected from the vehicle is insufficient to illuminate the shock boundary.

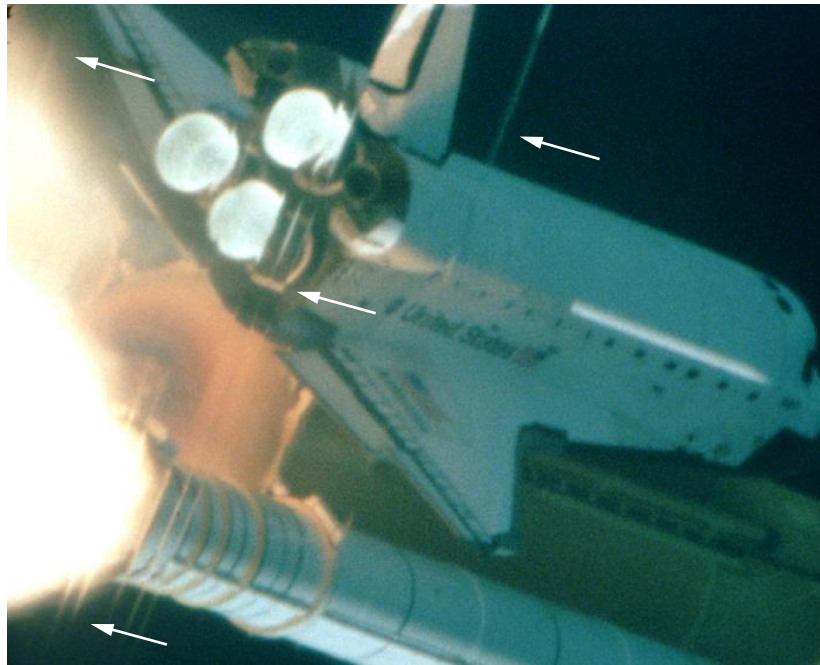


Figure 30. Multiple LODs visible.

### 4.4 Ripples in a Shock Boundary

Ripples in a shock boundary may be noted in the way that light is refracted. This is likely associated with the density change at the shock boundary, with the more dense side of the shock showing the typical distortion effect due to refraction and the less dense side showing little distortion.

Along the body flap (fig. 31), the refraction due to a shock boundary may be observed to be deflected toward the top of the image. The leftmost arrow points to a LOD where the body flap is deflected upward from the right side of the boundary. The right arrow points to a LOD where the body flap is deflected upward from the left side of the boundary. In this particular example, the two LODs noted are associated with a group that moves together and may be correlated to one particular shock boundary. However, there are also LODs that move in opposite directions that also exhibit this phenomenon and it is suspected, but unknown, whether these LODs are associated with separate shock boundaries.



Figure 31. Refraction direction illustrates ripples in the shock boundary.

Also at the edge of a shock boundary, a spread of minor ripples is observed (fig. 32). These two images are from the same LOD group and ostensibly from the same shock boundary. (The LOD group travels aft.) The cause of these minor ripples is unknown. Larger ripples of this same LOD group are noted at the SSME nozzle in (a).

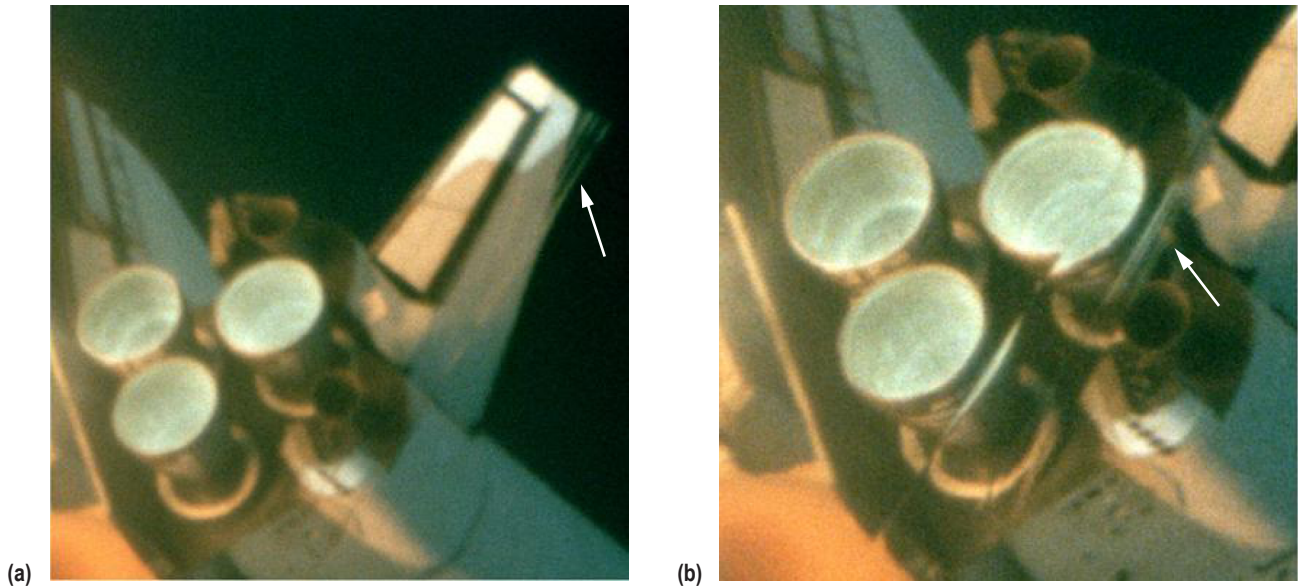


Figure 32. Minor ripples in the shock boundary: (a) Noted at a time prior to the time for (b).

#### 4.5 Other Observations of Linear Optical Distortions

Often during post-launch imagery evaluation, debris that falls aft of the vehicle during ascent can only be described as a light-colored object. When the vehicle is near SRB separation, only a few of the long-range tracking cameras have a resolution capable of distinguishing debris from the refractive effects of LODs. In figure 33, imagery from camera E207 during STS-116 captures the refractive effects of a shock boundary in the SRB plumes. Light from the SSMEs was also refracted and appeared as light-colored objects moving aft of the vehicle. Identification of shock boundaries helped to eliminate this observation as debris from the vehicle.

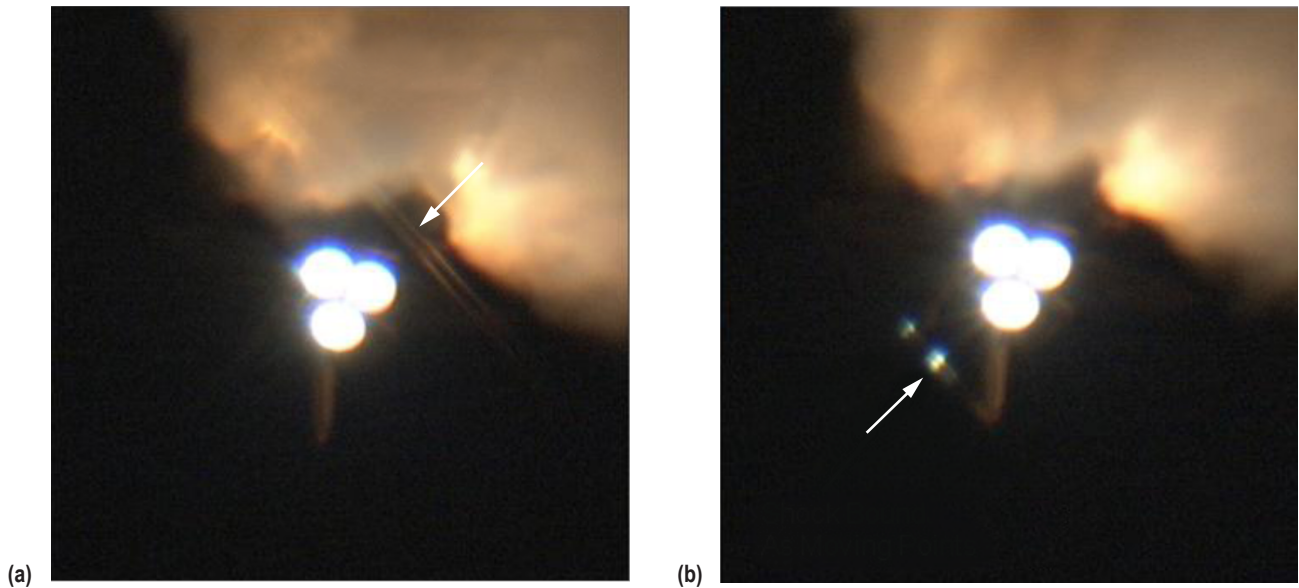


Figure 33. STS-116 SSME refraction: (a) Shock boundary visible in SRB plumes and (b) shock boundary visible as moving points of light.

Another example of this occurred on STS-107. As debris impacted the reinforced carbon-carbon (RCC) panels, there were multiple shock boundaries visible in the imagery from long-range tracking camera E212 (fig. 34). The shock boundaries were faint in the imagery due to the ambient lighting and resolution of the camera at that distance.

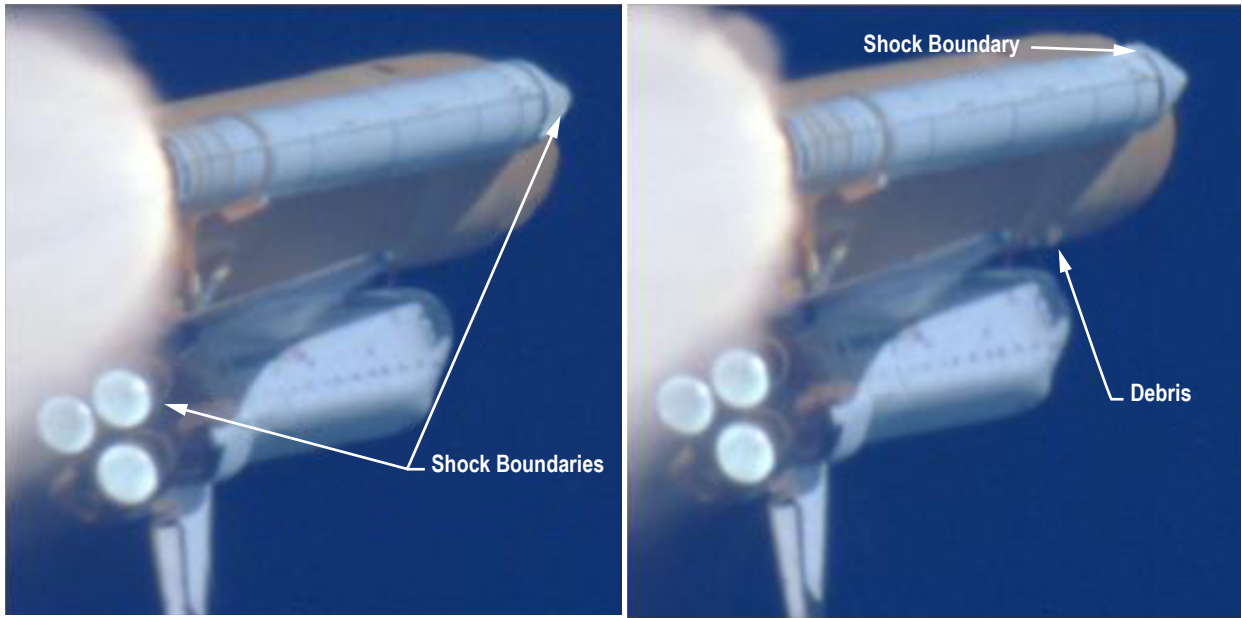


Figure 34. STS-107 shock boundaries (LODs).

## 5. DISCUSSION

Visualization of shock boundaries is often difficult in the field when tracking mobile objects. Often the only opportunity for visualization is the shock cone formation as the vehicle attains Mach 1.0. There are few Schlieren photographic visualizations of aircraft shock boundaries accomplished outside the laboratory that are available in the literature. This presentation illustrates the opportunities for shock wave visualization with good optical conditions made available using airborne WAVE and ground camera imagery assets and gives insight into the shock structures and time of occurrence in the SSV flow field. Movies of the LODs are available at the MSFC engineering photographic analysis Web site.<sup>4</sup>

For the photographic analyst, the knowledge of the presence of shock boundaries provides additional insight when evaluating mission imagery and in particular when making measurements of objects that may straddle a shock boundary.

This TM is predominantly qualitative but due to the excellent imagery captured by the SSP assets, a more quantitative investigation of the complex shock structures in flow field surrounding the SSV might be undertaken. Such an investigation might employ the relations between the shock density, Mach number, and index of refraction and a comparison with theoretical computations performed on these physical quantities at the separate shock boundaries observed.



## REFERENCES

1. Haering, E.A., Jr.; Ehernberger, L.J.; and Whitmore, S.A.: "Preliminary Airborne Measurements for the SR-71 Sonic Boom Propagation Experiment," *NASA TM-104307*, NASA Dryden Flight Research Center, Edwards, CA, September 1995.
2. Weinstein, L.M.; Stacy, K.; Vieira, Jr., G.J.; et al.: "Visualization and Image Processing of Aircraft Shock Wave Structures," First Pacific Symposium on Flow Visualization and Image Processing, Honolulu, Hawaii, 1997.
3. NSTS 08224, Rev. B: Program Launch and Landing Photographic Engineering Evaluation, NASA Marshall Space Flight Center, AL, February 27, 1997.
4. Engineering Photographic Analysis, Marshall Space Flight Center, AL, <<https://photo1.msfc.nasa.gov/msfc/>>, 2011.

REPORT DOCUMENTATION PAGE			Form Approved OMB No. 0704-0188		
<p>The public reporting burden for this collection of information is estimated to average 1 hour per response, including the time for reviewing instructions, searching existing data sources, gathering and maintaining the data needed, and completing and reviewing the collection of information. Send comments regarding this burden estimate or any other aspect of this collection of information, including suggestions for reducing this burden, to Department of Defense, Washington Headquarters Services, Directorate for Information Operation and Reports (0704-0188), 1215 Jefferson Davis Highway, Suite 1204, Arlington, VA 22202-4302. Respondents should be aware that notwithstanding any other provision of law, no person shall be subject to any penalty for failing to comply with a collection of information if it does not display a currently valid OMB control number.</p> <p><b>PLEASE DO NOT RETURN YOUR FORM TO THE ABOVE ADDRESS.</b></p>					
1. REPORT DATE (DD-MM-YYYY) 01-01-2011		2. REPORT TYPE Technical Memorandum		3. DATES COVERED (From - To)	
4. TITLE AND SUBTITLE  Direct Visualization of Shock Waves in Supersonic Space Shuttle Flight			5a. CONTRACT NUMBER		
			5b. GRANT NUMBER		
			5c. PROGRAM ELEMENT NUMBER		
6. AUTHOR(S)  J.M. O'Farrell* and T.J. Rieckhoff			5d. PROJECT NUMBER		
			5e. TASK NUMBER		
			5f. WORK UNIT NUMBER		
7. PERFORMING ORGANIZATION NAME(S) AND ADDRESS(ES) George C. Marshall Space Flight Center Marshall Space Flight Center, AL 35812			8. PERFORMING ORGANIZATION REPORT NUMBER  M-1304		
9. SPONSORING/MONITORING AGENCY NAME(S) AND ADDRESS(ES) National Aeronautics and Space Administration Washington, DC 20546-0001			10. SPONSORING/MONITOR'S ACRONYM(S) NASA		
			11. SPONSORING/MONITORING REPORT NUMBER NASA/TM-2011-216455		
12. DISTRIBUTION/AVAILABILITY STATEMENT Unclassified-Unlimited Subject Category 35 Availability: NASA CASI (443-757-5802)					
13. SUPPLEMENTARY NOTES Prepared by the Spacecraft & Vehicle Systems Department, Engineering Directorate *United Space Alliance, 555 Discovery Drive Northwest, Huntsville, AL 35806-2809					
14. ABSTRACT  Direct observation of shock boundaries is rare. This Technical Memorandum describes direct observation of shock waves produced by the space shuttle vehicle during STS-114 and STS-110 in imagery provided by NASA's tracking cameras.					
15. SUBJECT TERMS  space shuttle, shock wave, visualization, optics, refraction, tracking camera, WB-57					
16. SECURITY CLASSIFICATION OF:			17. LIMITATION OF ABSTRACT	18. NUMBER OF PAGES	19a. NAME OF RESPONSIBLE PERSON
a. REPORT	b. ABSTRACT	c. THIS PAGE			STI Help Desk at email: help@sti.nasa.gov
U	U	U	UU	32	19b. TELEPHONE NUMBER (Include area code) STI Help Desk at: 443-757-5802



National Aeronautics and

Space Administration

IS20

**George C. Marshall Space Flight Center**

Marshall Space Flight Center, Alabama

35812